4ICEGE Thessaloniki-GREECE 2007

4th International Conference on
Earthquake Geotechnical Engineering
June 25-28, 2007
Paper No. 1196

SHAKING TABLE EVALUATION OF DYNAMIC SOIL PROPERTIES

Matthew DIETZ [1], David MUIR WOOD[2]

ABSTRACT

The design and performance of a plane-strain experimental apparatus for evaluating fundamental dynamic properties of soils at low stress levels is described. The apparatus, named a shear stack, works in conjunction with a shaking table and consists of a flexible hollow box in which a test soil is deposited. The dynamic performance of the apparatus is verified by filling with a dry sand and comparing the response to lateral base acceleration with that predicted by the Hardin & Drnevich (1972) hyperbolic stress-strain relationship. The apparatus satisfactorily replicates the idealized free-field response across a wide range of strain.

Three techniques have been employed to evaluate the shear stiffness G and damping D using apparatus similar in form to the shear stack. Each utilizes a different excitation motion: random (Dar, 1993), pulse (Fishman et al., 1994) or sinusoidal (Brennan et al., 2005). Here, these three techniques are compared across a wide range of shear strain γ using dry Leighton Buzzard 14-25 (LB 14-25) sand. Shear stack data are contrasted with the relevant Seed & Idriss (1970) G-D-γ curves and Cavallero et al.'s (2001) LB 14-25 resonant column test data. Trends are generally as expected. It is concluded that fundamental dynamic soil properties at low stress levels can be evaluated quickly and at low cost by shear stack testing.

Keywords: Sand, Laboratory, Shear, Modulus, Damping, Shaking table.

INTRODUCTION

The hysteretic response of soil to cyclic shear stresses can be evaluated with reference to two fundamental parameters: shear modulus G and damping factor D. Each is usually expressed as a function of shear strain, γ. The G-D-γ curves required for numerical analyses of seismic geotechnical problems are normally obtained via element tests. At very low stress levels, instrumentation resolution and loading system limitations generally cause such tests to dysfunction. Low stress information is then extrapolated from data acquired at higher confining pressures. As an alternative, dynamic soil properties can be measured on a shaking table using a purpose designed soil container. The literature presents three techniques for evaluating the evolution of shear modulus and damping with shear strain using such shaking table soil containers. Each utilizes a different excitation motion: random (Dar, 1993), pulse (Fishman et al., 1994) or (near) sinusoidal (Brennan et al., 2005). Herein, these methodologies are for the first time contrasted using a newly built soil container. The advantages of each are discussed and practical considerations for their use are given.

Shaking table soil containers

Over the past forty years, the use of shaking table soil containers has become commonplace. Both single-gravity and centrifuge containers have been developed to tackle a wide variety of geodynamic

[1] Research Associate, Department of Civil Engineering, University of Bristol, UK, Email: m.dietz@bristol.ac.uk
[2] Dean, Faculty of Engineering, University of Bristol, UK.

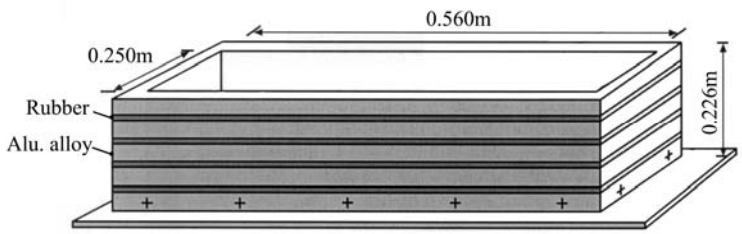

Figure 1. Zeng & Schofield's (1996) Equivalent Shear Beam soil container.

problems: soil-structure interaction, liquefaction, dynamic bearing capacity, slopes and embankments, piles, retaining walls. Regardless of this prevalence, containers are rarely used to obtain dynamic soil properties despite some potential advantages over conventional element tests. Sample sizes are limited only by the payload of the shaking table and can be much larger than those of element tests. Larger volumes of soil may better represent average field conditions. Additionally, the operative strain range is ultimately governed by the performance capabilities of the shaking table and can be relatively wide.

Containers generally consist of hollow boxes secured at their base to a shaking table and filled with a test soil. Boundary effects induced by the container walls must be minimized according to the modeling application. To model liquefaction, for example, the large lateral displacements associated with a liquefied soil must be unimpeded. Thus, the 'laminar box' was devised (e.g. Hushmand et al., 1988, Ueng et al., 2006). These containers are constructed from a stack of stiff rings each capable of independent and unrestrained lateral displacement giving the box negligible shear stiffness. Internal walls of the rings are made smooth to restrict boundary shear stresses.

When liquefaction is not of interest boundaries must be both frictional and flexible. For instance, Zeng & Schofield's (1996) Equivalent Shear Beam (ESB) centrifuge container, Figure 1, has roughened internal walls to enable shear stress transmission. It was constructed from an alternating stack of aluminium alloy and rubber rings for flexibility. The composite shear stiffness of the ESB was tuned to the dynamic stiffness of a test soil by careful detailing of the rubber layer thickness. This design specification is rather restrictive since soil-stiffness degradation ensures it can be achieved at only a single level of seismic excitation. For other soils and other levels of excitation the ESB malfunctions by either constraining or enhancing the dynamic lateral soil displacements.

Crewe et al. (1995) developed a more versatile soil container named a 'large shear stack'. Their design objective was that the test soil, not the stack, would drive the system response. To this end, the shear stiffness and inertia of the stack were minimised. No experimental verification of Crewe et al.'s (1995) stack has yet been presented. However, a performance evaluation of its smaller precursor is available. The hollow aluminium rings of Dar's (1993) shear stack are, like the ESB of Figure 1, separated by solid rubber rings giving it a fundamental frequency when empty of 12Hz. Dar (1993) used his stack to investigate the degradation of shear stiffness and damping of a dry sand deposit via resonant testing (described later. His data are presented in Figure 6.) A limitation of Dar's (1993) apparatus is that at higher strains the experimentally derived stiffness is higher than expected. Crewe et al (1995) reasoned that although the soil suffers from stiffness degradation, the stack remains elastic and, as a result, increasingly dominates the response.

EXPERIMENTAL HARDWARE

The new small shear stack

The latest shear stack incarnation is a direct descendant of Crewe et al.'s (1995) apparatus. However, it is closer in size to Dar's (1993) small shear stack: 1.2m long as opposed to 5m, 0.55m wide as opposed to 1m, and 0.8m deep as opposed to 1.2m, significantly reducing the costs and timescales associated with testing. Design details are presented in Figure 2.

The apparatus consists of eight aluminium rings, rectangular in plan, which are stacked alternately with rubber sections. The rubber sections span only the end-walls of the stack, not the side-walls, giving a fundamental frequency when empty of 6Hz, significantly less than Dar's (1993) apparatus. The aluminium rings are constructed from box section to minimise inertia. The stack is secured to the shaking table by its base and shaken horizontally lengthways (in the *y* direction). Its floor is roughened to aid the transmission of shear waves; the internal end walls are similarly treated to enable complementary shear stresses. The internal side walls are lubricated for plane strain. Not pictured in Figure 2 are the rigid steel restraining frame and the system of bearings used to prevent unwanted motion in the *x* and *z*-directions.

The idealized test soil response to base acceleration has been presented elsewhere and is as depicted in Figure 2(c). Vertically propagating shear waves induce shear stresses within a test soil. Normal stresses are kept constant. Lateral deflection *u* of the soil column in the *y*-direction is caused by shear deformation. The shear stress at depth *d* is the product of the soil density ρ and the integral of lateral acceleration through the overlying soil. Given surface acceleration $\ddot{u}_{d=0}$ and acceleration $\ddot{u}_d$ at depth *d*, first-order finite difference approximations for the shear stress τ'_{zy} and shear strain γ_{zy} at time *t* are:

$$\tau'_{zy}(d,t) = \rho d\left(\ddot{u}_d(t) + \ddot{u}_{d=0}(t)\right)/2 \quad (1)$$

$$\gamma_{zy}(d,t) = \left(u_d(t) - u_{d=0}(t)\right)/d \quad (2)$$

Shaking table

The new small shear stack is to be used in conjunction with the shaking table at the Bristol Laboratory for Advanced Dynamic Engineering (BLADE), the main facility for experimental research into earthquake engineering at the University of Bristol. It consists of a 3m by 3m cast aluminium seismic platform capable of carrying a maximum payload of 21 tonnes. The platform is mounted on a 100 tonne isolating block and is driven horizontally and vertically by eight 300mm stroke, 70kN servo hydraulic actuators giving full control of motion of the platform in all six degrees of freedom simultaneously. Hydraulic power for the actuators is provided by five pairs of hydraulic pumps capable of delivering 900 litre/min at a working pressure of 230 bar. The table operates up to 100Hz.

The high specification of the BLADE shaking table allows for great subtlety in loading. Motion amplitude can be varied by the simple application of a scalar multiplier to the excitation waveform. This has particular relevance for shear stack testing. The lateral acceleration of the shaking table can be employed as the control parameter that governs the level of strain experienced by the test soil.

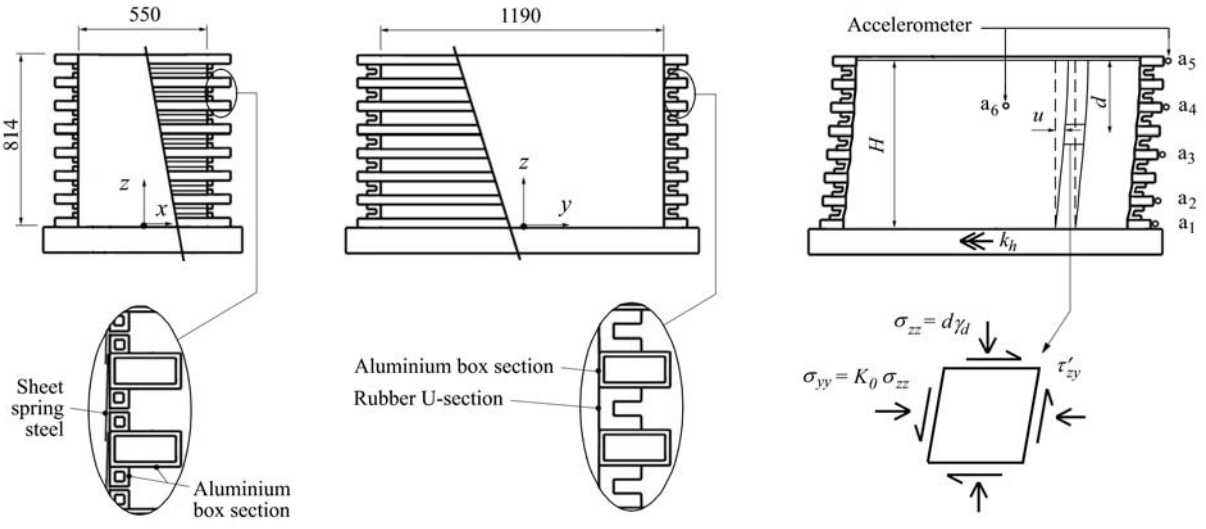

Figure 2. The shear stack: (a) cross section; (b) long section; (c) long section during testing.

Sand

Dry Leighton Buzzard (14-25) sand is used in all tests. This sand has sub-rounded particles with mean particle size 0.8mm.The test sand is deposited within the shear stack using a dry pluviation technique. A 300kg drum of the test material is inverted 1.2m above the base of the shear stack. On releasing a valve, the sand flows through a funnel attached to the underside of the suspended drum. The flow is constricted by an adjustable aperture at the tip of the funnel. This aperture provides the primary control on the resulting sample density (Miura & Toki, 1982). On leaving the funnel, the sand flows into a flexible tube 1m in length and 50mm diameter allowing the flow to be directed. Layers of 100mm depth are poured, the flow is stopped, and the drum is raised by 100mm. Preliminary tests reveal that an aperture of 15mm produces a void ratio of 0.6 and density 1.69 tonne/m^3. It takes around three hours to deposit the 800mm depth (nearly 900kg mass) of sand required to fill the shear stack. It is feasible to set up the experimental apparatus, deposit the test soil and test that same day.

The limiting shear modulus for the deposit is calculated using Hardin & Drnevich's (1972) empirically derived relationship for sands:

$$G_0(d) = \frac{3230(2.973 - e)^2 \sqrt{\sigma'_m}}{1 + e} \tag{3}$$

Here, σ'_m is the mean effective confining stress. Stroud (1971) measured K_0 values of 0.445 and 0.46 for dense and loose LB 14-25 sand whilst developing the Cambridge Simple Shear Apparatus. At the base of the shear stack, taking K_0 as 0.45 (the average of Stroud's measurements), σ'_m is calculated as 8.4kN/m^2 rendering G_0 at same location as 33MPa.

Instrumentation

As depicted in Figure 2(c), six accelerometers are used to record the lateral response in the *y*-direction. The accelerometers are of type 141a manufactured by Setra. These instruments are high output capacitance type with inbuilt pre-amplifiers which operate over a frequency range of 0 to 3000Hz. Five sensors are secured at different *z*-ordinates to the external walls of the stack. The final sensor is encased within an aluminium box with roughened external faces and embedded during sample deposition centrally within the deposit at a *z*-ordinate of 0.55m. The box dimensions are designed to give an average mass density equivalent to that of the sand deposit.

To reduce noise, data signals from the instruments are passed through a low pass Butterworth filter set to 80Hz. Data are acquired at a rate of either 200Hz (sinusoidal and random excitation) or 1000Hz (pulse excitation). To aid data processing, acquisition is initiated a few seconds prior to the start of any movement of the shaking table and ends a similar amount of time afterward. This gives flat tails to the measured time histories.

DATA PROCESSING

Raw accelerometer data are treated as follows. Data have any DC offset removed by deducting the average of the first 50 sampled data points from the entire time history producing a voltage time history distributed around 0V. Multiplication by the relevant accelerometer calibration statistic then converts the voltages to accelerations. To calculate shear strains, accelerations must be converted into displacements.

Acceleration data are integrated with respect to time using the trapezoidal method to produce velocities. Integrated data are generally associated with a drift error. To compensate, the data are filtered using a high-pass Butterworth filter set at a suitably low value. 0.3Hz is used. Phase distortion is negated by multiple application of the filter. After primary application, the filtered history is reversed in time and passed back through the filter. Subsequent reversal gives a filtered time history free from phase distortion. Trapezoidal integration of the calculated velocities followed by forward-

reverse filter sequence is undertaken to produce displacements. A close match between the second derivatives of the displacement (easily calculated using a 2nd order Savitzky-Golay smoothing filter) and the original acceleration measurement gives confidence in the integration/filtering process. Displacements derived in this manner are relative to a stationary point remote from the shaking table. Relative displacement time histories are calculated by subtracting the table displacement history (derived from sensor a_1) from the time history in question.

Equations 1 and 2 rely on the measurement of surface acceleration. In practice, this is difficult to achieve since an accelerometer needs to remain in good contact with the soil. Furthermore, reliable acceleration measurement within the shear stack sample's uppermost horizons is complicated by a large stiffness discontinuity between the lightly stressed sand and the embedded instrumentation. For these reasons, Brennan et al. (2005) linearly extrapolated the accelerations recorded deeper within a soil deposit to the surface. Here, surface accelerations are calculated in similar fashion by making reference to sensors a_1 and a_6 (see Figure 2(c)):

$$\ddot{u}_{d=0}(t) = \ddot{u}_{d=H}(t) + H\left(\ddot{u}_{z=0.550}(t) - \ddot{u}_{d=H}(t)\right)/0.550 \tag{4}$$

PERFORMANCE ASSESSMENT

The performance of the shear stack can be assessed by adapting the design methodology of Zeng & Schofield's (1996) ESB soil container.

The deformation of a soil element in a soil column subjected to lateral base shaking depends on the stress-strain relationship of the soil. Zeng & Schofield (1996) utilized the Hardin & Drnevich (1972) hyperbolic stress-strain relationship to describe the idealized soil response. This non-linear elastic model relates shear strain γ_{zy} to shear stress τ'_{zy} using limiting values of shear stiffness G_0 and shear stress τ'_{max}:

$$\gamma_{zy}(d,t) = \tau'_{\max}\tau'_{zy}(d,t)/\left(G_0\tau'_{\max} - G_0\tau'_{zy}(d,t)\right) \tag{5}$$

Integration of γ_{zy} across the soil depth d gives the lateral displacement u_d. G_0 can be calculated from Equation 3; τ'_{zy} from Equation 1 at defined acceleration magnitudes. An expression for τ'_{max} can be derived from a consideration of Mohr's circles for a soil element of density ρ and strength ϕ' undergoing lateral acceleration (Zeng & Schofield, 1996):

$$\tau'_{\max}(d) = \frac{\rho g d}{2}\sqrt{\left(\sin\phi' + K_0\sin\phi'\right)^2 - \left(1 - K_0\right)^2} \tag{6}$$

The measured peak lateral deflections of the full ESB container subjected to three magnitudes of earthquake are compared with the idealized response in Figure 3(a) (taken from Zeng & Schofield, 1996). At low excitation levels, the stiffness of the soil is higher than that of the ESB and so inertia of the ESB drives the deflections upwards. At high excitations, the stiffness of the soil is lower than that of the ESB and the ESB constrains deflections. At the design earthquake, stiffness and deflection of the soil and ESB match.

The performance of the shear stack can be assessed by comparing the deflections of its end wall with the response predicted by the Hardin & Drnevich (1972) model. The assessment is valid at low to medium excitation levels, when induced shear stresses τ'_{zy} are less than the limiting magnitude given by Equation 6. At higher acceleration levels, Equation 5 breaks down. For LB 14-25, this occurs at a shaking table acceleration of around 0.38g.

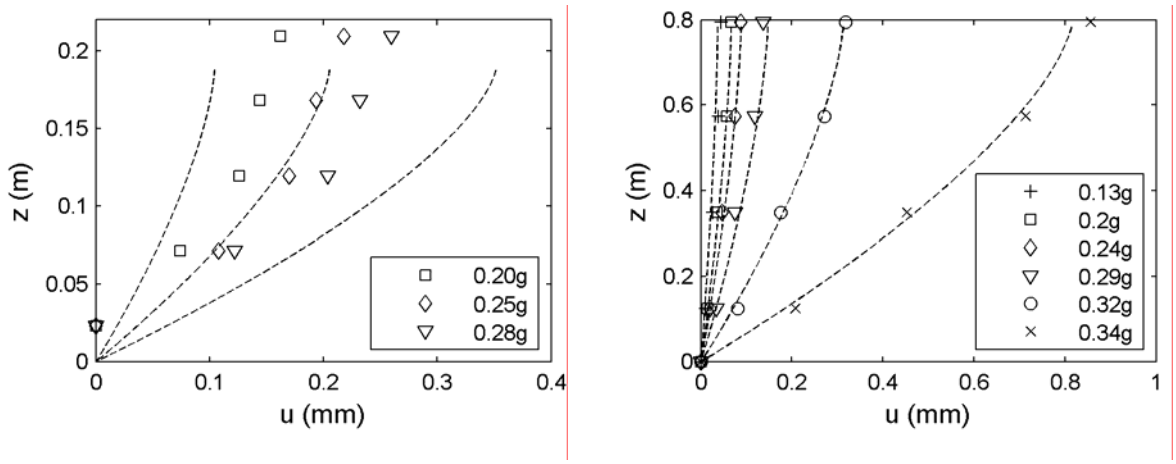

(a) **(b)**

Figure 3. End-wall deflections (symbols) compared to the idealized response calculated at equivalent acceleration levels (dashed lines): (a) Zeng and Schofield's (1996) ESB; (b) the shear stack.

The full shear stack was excited using a 10Hz sinusoidal waveform. The waveform was ramped up over the course of 10 oscillations, held at constant amplitude for 20 oscillations, and ramped down over 10 oscillations. A typical acceleration and displacement response is presented in Figure 4. A single cycle of response was selected (Figure 5) from which peak displacements of the shear stack's end walls were extracted. The procedure was repeated at six different amplitudes of excitation.

Peak deflection data are plotted in Figure 3(b) alongside the Hardin & Drnevich (1972) predictions. The response is adequately predicted at all excitation magnitudes. Unlike the ESB, it appears that the inertia driven phenomenon of increased deflections when the container to soil stiffness ratio is less than unity is not apparent. This is presumably due to the comparatively small inertia forces induced by the stack's hollow aluminium rings.

In summary, low magnitudes of soil container stiffness and inertia are necessary when the requirement is to test across a wide range of strain. With low stiffness and low mass, the shear stack response is as predicted up until failure.

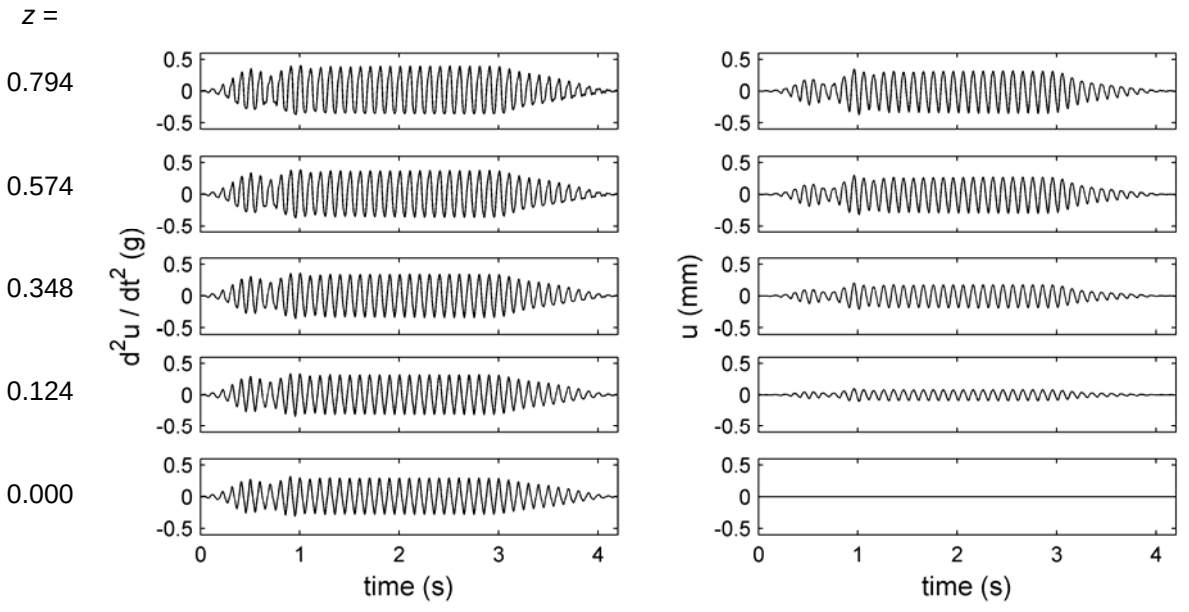

(a) **(b)**

Figure 4. Sine dwell testing of a full stack: (a) measured accelerations; (b) derived displacements.

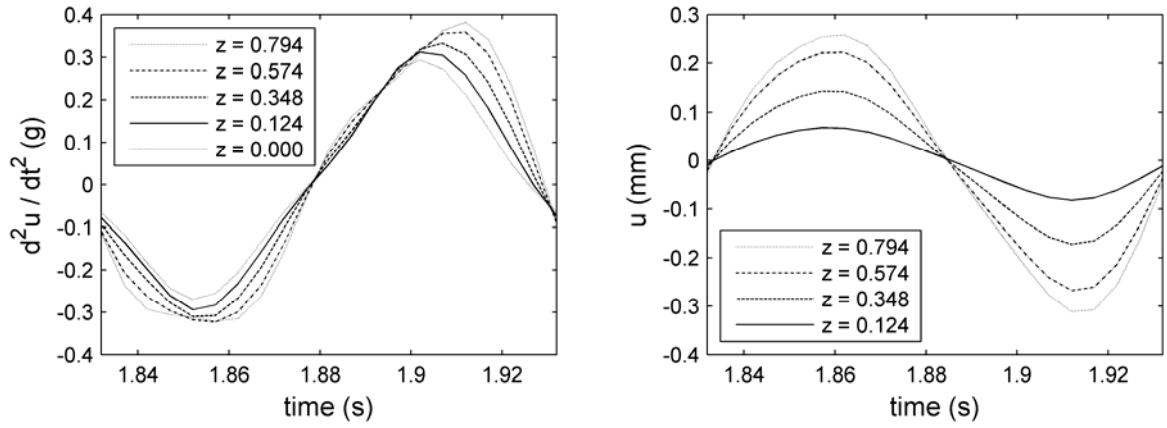

(a) **(b)**

Figure 5. Typical single cycle time history: (a) acceleration; (b) displacement

EVALUATION OF DYNAMIC PROPERTIES

The literature presents three techniques capable of estimating shear modulus *G* and damping *D* from shaking table soil containers. Each makes use of a different horizontal excitation waveform: random, pulse or sinusoidal. Dar (1993) used the frequency response functions derived during random excitation tests to extract the dynamic soil properties. Fishman et al. (1995) directly measured shear-wave travel times during pulse tests but stopped short of calculating shear moduli from the interpreted velocities. Brennan et al. (2005) estimated the dynamic soil properties via a geometric analysis of the hysteretic response recorded in the centrifuge using a sinusoidal type excitation. Here, the new small shear stack and the LB14-25 test soil are used to compare these three techniques.

Data are evaluated by comparison with two data sets. The first consists of the Seed & Idriss (1970) curves that chart the evolution of G / G_0 and D with strain level. These empirically derived curves for sands (solid lines) and their limits (dashed lines) are shown in Figure 6. The curves represent 'average' response since they are derived from a wide variety of test procedures and test soils. The second data set is taken from Cavallaro et al. (2001) who conducted a series of resonant column tests using LB 14-25 as obtained from BLADE. Tests were conducted at stress levels spanning between 49kPa and 151kPa and between strains of 0.0002 and 0.055%, limits imposed by the test apparatus. The void ratio spanned between 0.563 and 0.660. Their data are summarized as dash-dot trendlines in Figure 6. The stiffness degradation recorded by Cavallaro et al. (2001) is akin to the Seed & Idriss (1970) curve. There is some discrepancy in the trend for damping, particularly towards higher strain levels.

Random excitation

A digital spectrum analyzer (of type Advantest series R9211) is used to measure the resonant properties of the test sand within the shear stack. A random signal of bandwidth 1-50Hz from the analyser's inbuilt signal generator excites the shaking table in the *y*-direction. Frequency response functions (FRFs) are calculated by normalizing the output of sensor a_5 by the output of sensor a_1 in the frequency domain. Noise effects are minimized by analyzing 32 four second data segments and averaging the results. A Hanning window is used. The nominal 128 second test duration is actually a minimum value due to the disqualification of bad data segments wherein the voltages from the sensors saturate the analyzer.

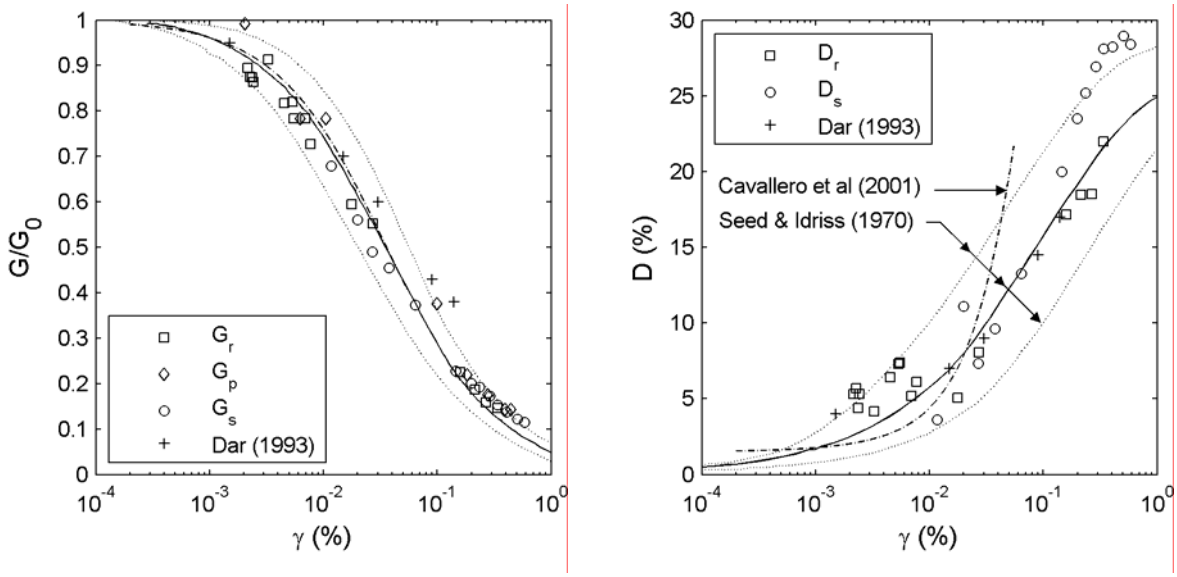

(a) **(b)**

Figure 6. The evolution of *G* and *D* with shear strain.

Typical frequency domain results are shown in Figure 7. FRFs are dominated by a single resonant peak corresponding to the first shear mode of the soil layer response. The peak reduces in height, increases in width and migrates to lower frequencies with increases in excitation indicating reduced amplification, increased damping and a softening of response at increased strain levels. These trends are supported by the decreasing gradient of the phase plots of Figure 7(b). No other modes of soil response exist within the 1-50Hz frequency band. FRFs display a second resonant peak at 20Hz smaller in magnitude and comparatively insusceptible to changes in excitation. It represents a table (oil column) resonance and is not representative of the test soil response.

Resonant frequencies f and modal damping values D_r are obtained using a curve fitting algorithm that derives the complex pole value for each resonant peak. Noting that the first mode of response corresponds to a shear wave of length $4H$, the resonant frequencies can be converted to shear stiffness G_r with the following relation:

$$G_r = 16\rho H^2 f^2 \tag{8}$$

G_r represents an average value for the test sand. It has been normalized by $(G_o)_{d=H}$ / 2 (16.5MPa) for plotting in Figure 6. The associated strain levels are derived by double integration of the acceleration time histories measured by sensor a_5.

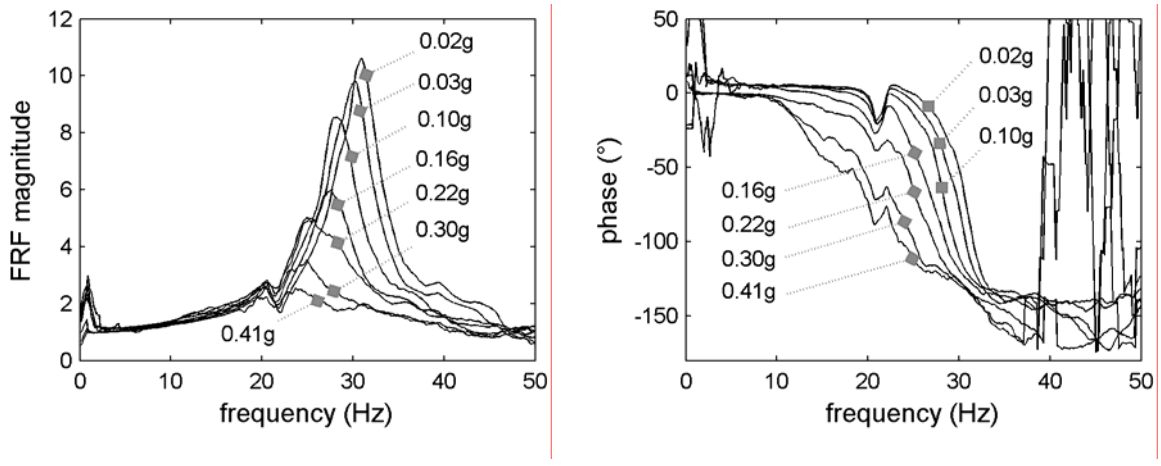

(a) **(b)**

Figure 7. FRFs at different (RMS) excitation accelerations: (a) magnitude; (b) phase.

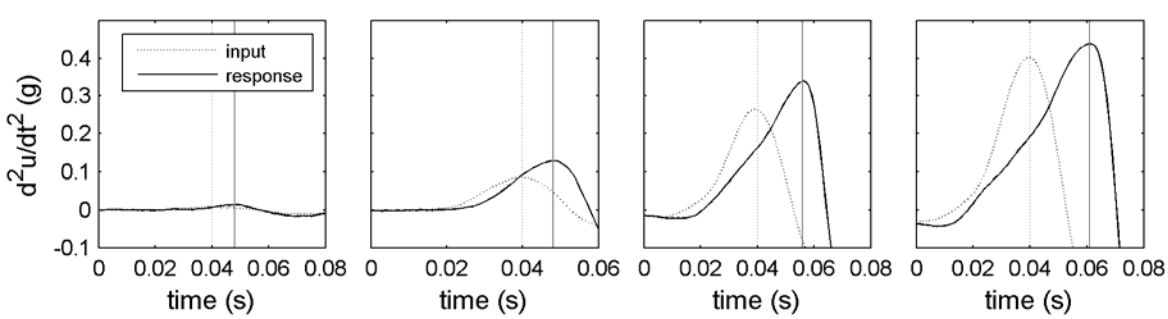

Figure 8. Time histories for pulse tests of increasing magnitude.

Pulse testing

The travel time t of a shear wave propagating vertically through the shear stack can be determined using a pulse type excitation and subtracting the time of peak base response from the time of peak surface response. For homogeneous soil deposits of density ρ and depth H, travel times can be converted to shear moduli with the following relationship:

$$G_p = \rho H^2 / t^2 \tag{7}$$

At low magnitudes of strain, shear-wave travel times are small. Data analysis is aided by maximizing the vertical distance between the measurement points and employing a sufficiently high rate of data acquisition. Equation 7 dictates that at small strain (G_0 = 16.5MPa) a shear wave will take 8 milliseconds to travel through the deposit. Thus, travel times are calculated using the data generated by sensors a_1 and a_5 sampled at a rate of 1000Hz.

A 10Hz half sine wave excitation pulse is utilized. A selection of typical time-history results is displayed in Figure 8 wherein the lag of the response (a_5) behind the excitation (a_1) increases with excitation magnitude. Travel times are converted to shear moduli using Equation 7 and, noting that G_p is an average for the sand deposit, are normalized by $(G_0)_{d=H}$ / 2 (16.5MPa) for plotting in Figure 6. The associated strain levels are derived by double integration of the acceleration time histories recorded by sensor a_5. It was intended to obtain estimates of damping D_p from the decrement of free vibration occurring immediately after pulse testing. However, the shaking table had difficulty reproducing the sudden halt at the end of the pulse but instead converged on its zero position via a number of cycles of successively reducing magnitude. As a result, extraneous excitation was applied invalidating free-vibration analysis.

Sine dwell excitation

Dynamic soil properties are here derived from a geometrical analysis of hysteresis loops. To the authors' best knowledge, this is the first time this has been attempted at single gravity.

The test sand is subjected to thirteen 10Hz sine dwells of successively increasing amplitude. For each test, a single cycle of excitation is extracted from the acceleration time histories (Figure 5). Shear stresses and strains are calculated for an element of sand at depth d = 0.4m using Equations 1 and 2. Figure 9 presents hysteresis loops for eight of the tests. As expected, increases in acceleration level cause the hysteresis loop to flatten and broaden indicating both a degradation of stiffness and an increase in damping with strain level.

Brennan et al.'s (2005) methodology for extracting shear modulus G_s and damping D_s is depicted for an idealized hysteresis loop in Figure 10. For hysteresis loops measured either in the centrifuge (Brennan et al., 2005) or at single gravity (Figure 9), the limiting values of τ'_{zy} and γ_{zy} generally do not coincide. Despite this, Brennan et al. (2005) found the equations of Figure 10 give the best representative values of G_s and D_s.

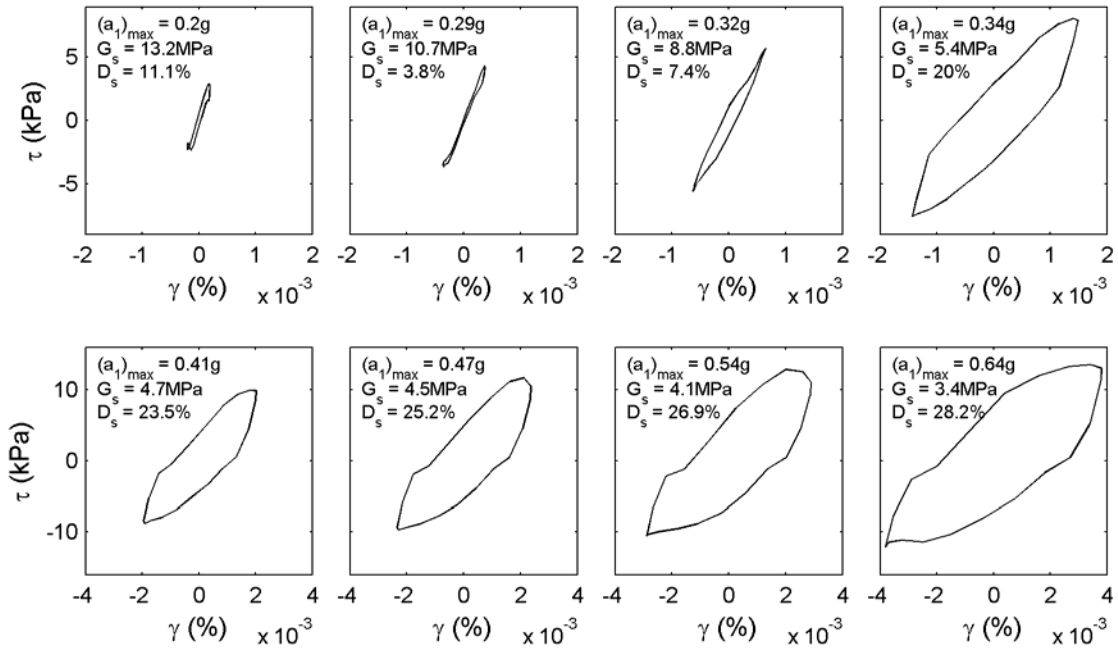

Figure 9. Hysteresis loops at various excitation magnitudes.

Thirteen hysteresis loops at successively increasing excitation magnitudes are analysed for G_s and D_s. G_s values have been normalized by the G_0 value obtained using Equation 3 at $d = H/2$ to enable plotting in Figure 6. Peak shear strains are obtained directly from the hysteresis loop plots.

DISCUSSION

Before data are discussed, the practicalities of each test methodology are contrasted.

Of the three methodologies it is pulse testing requires the least effort. Signal processing is comparatively simple and test durations are short. However, test interpretation is subjective in that the shear wave arrival times are ascertained by the manual comparison of time histories. Additionally, data acquisition hardware must be capable of providing the necessary data sampling rates, much higher than those usually employed in earthquake engineering applications. The most demanding signal processing is associated with sine dwell testing which provides ample opportunity for error. The frequency domain analysis of the random excitation tests is a good deal more straightforward, particularly if a spectrum analyzer is available. On grounds of practicality, it is this test methodology which must be recommended.

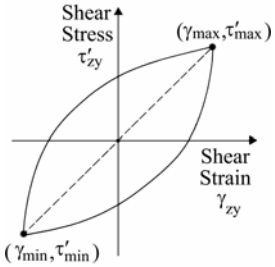

$$G_s = \left(\tau'_{\max} - \tau'_{\min}\right) / \left(\gamma_{\max} - \gamma_{\min}\right)$$

$$D_s = \frac{1}{4\pi} \times \frac{\oint \tau'_{zy} d\gamma_{zy}}{\left(\tau'_{\max} - \tau'_{\min}\right)\left(\gamma_{\max} - \gamma_{\min}\right)/8}$$

Figure 10. Dynamic soil properties from the geometry of an idealised hysteresis loop

There are occasions when random excitation tests may not be appropriate. It is well known that sands can exhibit volumetric change when sheared. For the medium-dense test soil, seismic excitation produces a net contraction of the deposit evidenced as settlement of the sample surface. The test soil void ratio decreases resulting in an increased sample density. Strictly, these variations should be reflected in the calculations for shear stress and stiffness. For the test soil in question, measured contractions had negligible influence on other parameters and volumetric change was disregarded. Nevertheless, if substantial settlement does occur, any derived dynamic soil properties should be related to average soil properties over the test. The amount of settlement is dependent on the magnitude and duration of the shear strain. For tests of equivalent shear strain magnitude, the prolonged duration of the random excitation test maximizes settlement while the short duration of the pulse test minimizes settlement. If a deposit must be preserved for future modeling application and yet its dynamic properties are required, it is recommended that the pulse excitation tests be employed.

Figure 6(a) illustrates that shear stack data can be represented by the standard G-γ curve regardless of the testing technique employed. The correlation is most satisfying with the random test data. This is because the Seed & Idriss (1970) curve represents an average response. Of the three stiffness parameters derived here, G_r best represents an average value for the test sand since it is derived from large amounts of averaged broadband data. Derived from a single measurement of travel time, G_p exhibits the poorest correlation with the standard curve.

There is a tendency for test data to lie above the standard G-γ curve at strains in excess of 0.2%. Dar's (1993) data exhibited a similar trend at strains above 0.02% and are reproduced in Figure 6 for comparison. Crewe et al (1995) surmised that at these strain levels the soil has softened sufficiently for the soil container to interfere with system response. The stiffness of the new shear stack is half the magnitude of Dar's (1993). By softening the soil container, its operative strain range is widened.

Reliable damping data are more elusive. For the series of tests presented herein, D_p values are unobtainable due to extraneous (post-pulse) vibration of the shaking table. In future, iterative matching software (Crewe, 1998) should be employed to achieve a better match between excitation applied by the shaking table and the desired pulse waveform. Only then might D_p measurements become attainable.

Figure 6(b) shows that at small strain levels D_r has a tendency to lie above both the Cavallaro et al. (2001) and the Seed & Idriss (1970) trendlines. This may well be caused by the damping inherent in the rubber which gives the shear stack its flexibility. At increased strains, D_r values fall within the expected range. At high strains, D_s values tend to lie above the upper Seed & Idriss (1970) limit. It is unclear why this should be so. Clarity is not aided by the significant divergence between the Cavallaro et al. (2001) trendline and the Seed & Idriss (1970) trendline at medium strain levels. Further tests are required to understand the response of the shear stack at high strain magnitudes.

CONCLUSIONS

A shear stack that works in conjunction with a shaking table and is capable of evaluating the dynamic properties of test soils has been designed and built. Its walls are flexible so that when subjected to base shaking it shears along with the included soil deposit. The low stiffness and inertia of the stack widens its operative strain range. The dynamic response of the stack has been compared with the idealized response as predicted by the Hardin & Drnevich (1972) hyperbolic stress-strain relationship. The comparison is favorable at all magnitudes of excitation acceleration up until failure. It is concluded that the free-field condition is reproduced within the shear stack.

Three test techniques capable of characterizing the evolution of shear stiffness and damping with strain level have been compared. Each utilized a different excitation waveform: random, pulse or sinusoidal. Acquired shear stack data have been compared with published G-D-γ curves. The

degradation of shear modulus with shear strain experienced by the shear stack test soil agrees well with the expected trend regardless of the test technique employed. Dissimilarities at high strain levels are due to the shear stack interfering with the response of highly softened test soil. Reliable damping data are more elusive but trends are generally as expected. It is concluded that fundamental dynamic soil properties at low stress levels can be evaluated quickly and at low cost by shear stack testing.

AKNOWLEDGEMENTS

The tests presented here were performed as part of the New Methods of Mitigating the Seismic Risk of Existing Foundations (NEMISREF) project funded by the 5th framework of the European Commission.

REFERENCES

Brennan, A.J., Thusyanthan, N.I. & Madabhushi, S.P.G., "Evaluation of shear modulus and damping in dynamic shaking table tests," Journal of Geotechnical and Geoenvironmental Engineering, ASCE, 131, 12, 1488-1496, 2005.

Cavallaro, A., Maugeri, M. & Mazzarella, R., "Static and dynamic properties of Leighton Buzzard sand from laboratory tests," Paper 1.13, Proc. 4th Int. Conf. Recent Advances in Geotechnical Earthquake Engineering, San Diego, California, March 26-30, 2001.

Crewe, A.J., 'The characterization and optimization of earthquake shaking table performance,' PhD Thesis, University of Bristol, 1998.

Crewe, A.J., Lings, M.L., Taylor, C.A., Yeung, A.K. & Andrighetto, R. "Development of a large flexible shear stack for testing dry sand and simple direct foundations on a shaking table," European seismic design practice, Elnashai (ed), Balkema, Rotterdam, 1995.

Dar, A.R., "Development of a flexible shear stack for shaking table testing of geotechnical problems," PhD thesis, University of Bristol, 1993.

Fishman, K. L., Mander, J. B. & Richards Jr., R., "Laboratory study of seismic free-field response of sand," Soil Dynamics and Earthquake Engineering, 14, 33-43, 1995.

Hardin, B.O. & Drnevich, V.P., "Shear modulus and damping in soils," Journal of Soil Mechanics and Foundations Division, ASCE, 98, 7, 667-692, 1972.

Hushmand, B., Scott, R.F., & Crouse, C.B., "Centrifuge liquefaction tests in a laminar box," Geotechnique, 38, 2, 253-262, 1988.

Miura, S. & Toki, S., "A sample preparation method and its effects on static and cyclic deformation-strength properties of sand," Soils Fnds, 22, 1, 61-77, 1982.

Seed, H.B., Idriss, I.M., "Soil moduli and damping factors for dynamic response analysis," EERC report 70-10, University of California, Berkeley, 1970.

Stroud, M.A., 'The behaviour of sand at low stress levels in the simple shear apparatus,' PhD Thesis, University of Cambridge, 1971.

Ueng, T.S., Wang, M.H., Chen, M.H., Chen, C.H. & Peng, L.H., "A large biaxial shear box for shaking table test on saturated sand," Geotechnical Testing Journal, 29, 1, 1-8, 2006.

Zeng, X. & Schofield, A.N., "Design and performance of an equivalent-shear-beam container for earthquake centrifuge testing," Geotechnique, 46, 1, 83-102, 1996.